HHS Public Access

Author manuscript

J Pineal Res. Author manuscript; available in PMC 2016 September 01.

Published in final edited form as:

J Pineal Res. 2015 September ; 59(2): 190–205. doi:10.1111/jpi.12250.

Melatonin reverses H_2O_2-induced premature senescence in mesenchymal stem cells via the SIRT1-dependent pathway

Long Zhou[#1,2], **Xi Chen**[#1,2,3], **Tao Liu**[2], **Yihong Gong**[4], **Sijin Chen**[5], **Guoqing Pan**[1,2], **Wenguo Cui**[1,2], **Zong-Ping Luo**[1,2], **Ming Pei**[6], **Huilin Yang**[1,2], and **Fan He**[1,2]

[1]Orthopaedic Institute, Medical College, Soochow University, Suzhou, China

[2]Department of Orthopaedics, The First Affiliated Hospital of Soochow University, Suzhou, China

[3]School of Biology and Basic Medical Sciences, Medical College, Soochow University, Suzhou, China

[4]School of Engineering, Sun Yat-sen University, Guangzhou, China

[5]Nanfang Hospital, Southern Medical University, Guangzhou, China

[6]Stem Cell and Tissue Engineering Laboratory, Department of Orthopaedics, West Virginia University, Morgantown, USA

[#] These authors contributed equally to this work.

Abstract

Mesenchymal stem cells (MSCs) represent an attractive source for stem cell-based regenerative therapy, but they are vulnerable to oxidative stress-induced premature senescence in pathological conditions. We previously reported antioxidant and antiarthritic effects of melatonin on MSCs against proinflammatory cytokines. In this study, we hypothesized that melatonin could protect MSCs from premature senescence induced by hydrogen peroxide (H_2O_2) via the silent information regulator type 1 (SIRT1)-dependent pathway. In response to H_2O_2 at a sublethal concentration of 200 μM, human bone marrow-derived MSCs (BM-MSCs) underwent growth arrest and cellular senescence. Treatment with melatonin before H_2O_2 exposure cannot significantly prevent premature senescence; however, treatment with melatonin subsequent to H_2O_2 exposure successfully reversed the senescent phenotypes of BM-MSCs in a dose-dependent manner. This result was made evident by improved cell proliferation, decreased senescence-associated β-galactosidase activity, and the improved entry of proliferating cells into the S phase. In addition, treatment with 100 μM melatonin restored the osteogenic differentiation potential of BM-MSCs that was inhibited by H_2O_2-induced premature senescence. We also found that melatonin attenuated H_2O_2-stimulated phosphorylation of p38 mitogen-activated protein kinase,

Corresponding Author: Fan He, Ph.D., Orthopaedic Institute, Soochow University, No.708 Renmin Road, Suzhou 215007, Jiangsu, China. Telephone: +86-512-67781420; Fax: +86-512-67781165; fanhe@suda.edu.cn.

Conflicts of Interest

The authors declare no conflicts of interest.

Author Contributions

LZ, XC, and FH designed the research study; LZ, XC, TL, GP, WC, and FH performed the experiments; LZ, XC, SC, ZPL, HY, and FH analyzed the data; FH wrote the paper; YG and MP participated in the conception of the study and revision of the manuscript. All authors approve of the final version to be published.

decreased expression of the senescence-associated protein $p16^{INK4\alpha}$, and increased SIRT1. Further molecular experiments revealed that luzindole, a nonselective antagonist of melatonin receptors, blocked melatonin-mediated anti-senescence effects. Inhibition of SIRT1 by sirtinol counteracted the protective effects of melatonin, suggesting that melatonin reversed senescence in cells through the SIRT1-dependent pathway. Together, these findings lay new ground for understanding oxidative stress-induced premature senescence and open perspectives for therapeutic applications of melatonin in stem cell-based regenerative medicine.

Keywords

mesenchymal stem cells; melatonin; hydrogen peroxide; senescence; SIRT1

Introduction

Mesenchymal stem cells (MSCs), originally identified in bone marrow stroma [1], have attracted great interest for cell-based strategies for tissue engineering and regenerative medicine due to their capacity for self-renewal and multilineage differentiation [2]. In order to generate sufficient cells for therapeutic purposes, MSCs have to be expanded by passaging *in vitro*; however, propagation of MSCs *in vitro* is hampered by the fact that cells undergo a process of replicative senescence. Cellular senescence is a phenomenon in which MSCs gradually lose their proliferative ability and proceed to G1 cell cycle arrest [3]. In addition, it has been reported that MSCs subjected to oxidative stress may undergo a process of premature senescence [4]. Prematurely senescent MSCs feature characteristics of cells with replicative senescence, such as an enlarged and flattened cell shape, loss of proliferative potential, irreversible cell cycle arrest, and increased senescence-associated β-galactosidase (SA-β-gal) activity [5, 6]. More importantly, the multi-lineage differentiation potentials of MSCs into osteoblasts, chondrocytes, adipocytes, myocytes, and even cells of non-mesodermal origin, including hepatocytes and neurons [7, 8], are impaired if senescence is induced [9]. This challenge hinders clinical application of MSCs in tissue regeneration [10].

Reactive oxygen species (ROS) such as hydrogen peroxide (H_2O_2), hydroxyl radicals, and superoxide anion, induce oxidative stress and are responsible for DNA damage [11]. If DNA damage is not properly repaired, cells will progress into premature senescence or apoptosis. A moderate level of ROS is critical for various cellular processes, such as proliferation and differentiation [12]; however, excessive ROS in pathological conditions is deleterious and induces cell death or cellular senescence [13]. Recent studies demonstrated that both long-term intracellular accumulation of H_2O_2[14] and exogenous exposure to sublethal doses of H_2O_2 [15] could induce MSCs into premature senescence.

On the molecular level, cellular senescence has been associated with two major intracellular signaling pathways: the p53/p21 pathway and the p38 mitogen-activated protein kinase (MAPK)/$p16^{INK4\alpha}$ pathway [16]. The protein p21, a cyclin-dependent kinase inhibitor (CKI), triggers the onset of cell cycle arrest, which can be induced by p53 [17]. In addition, accumulation of $p16^{INK4\alpha}$ can inhibit cell growth and is known as an important cell cycle

inhibitor; it is also a typical biomarker of cellular senescence [18]. Recently, human silent information regulator type 1 (SIRT1), a member of the nicotinamide adenine dinucleotide (NAD^+)-dependent deacetylase protein family, has been shown to recover the process of senescence by increasing cell proliferation and reducing $p16^{INK4\alpha}$ expression in human diploid fibroblasts [19]. SIRT1 also plays an important role in cell growth and multi-lineage differentiation by deacetylating various transcription factors such as p53 and peroxisome proliferator-activated receptor γ (PPARγ) [20, 21].

Melatonin (*N*-acetyl-5-methoxytryptamine) is an indole amine that is secreted primarily from the pineal gland and has been verified at a high level in the bone marrow [22]. Many studies have demonstrated that melatonin regulates a variety of physiological functions, such as sleep promotion, circadian rhythms, and neuroendocrine actions [23]. Melatonin has well known antioxidant properties, including scavenging excessive free radicals and increasing the synthesis of intracellular antioxidant enzymes [24, 25]. Our previous studies demonstrated that melatonin protects MSCs from pro-inflammatory cytokines by decreasing ROS generation and enhancing superoxide dismutase activities [26-28]. Furthermore, melatonin has been shown to control the biological functions of terminally differentiated cells (articular chondrocytes) [29] and direct MSC lineage-specific differentiation [30]. Nevertheless, the effects of melatonin on the premature senescence of MSCS induced by oxidative stress have not been elucidated and the effects of melatonin on the SIRT1 signaling pathway had conflicting conclusions. Yu et al. [31] demonstrated melatonin-mediated protection on myocardial ischemia/reperfusion (MI/R) injury by activating SIRT1 in a receptor-dependent manner. Compelling evidence showed that melatonin treatment promoted cell cycle arrest by enhancing p53 acetylation in MCF-7 cancer cells [32]. Therefore, the underlying mechanism that melatonin employs to modulate SIRT1 and the cell cycle regulators in senescent MSCs needs to be fully elucidated.

The specific aim of this study was to investigate the effects of melatonin on premature senescence of MSCs in response to oxidative stress. A sublethal concentration of H_2O_2 was determined to induce premature senescence in MSCs and the effects of melatonin treatments were evaluated in senescent MSCs. We also evaluated whether melatonin could rescue the osteogenic differentiation potential of MSCs that was suppressed by premature senescence. The underlying mechanism involving melatonin receptors and the SIRT1 signaling pathway were investigated.

Materials and methods

Reagents and antibodies

BM-MSCs were purchased from the American Type Culture Collection (ATCC; Manassas, VA, USA). Tissue culture polystyrene plates and flasks were purchased from Costar (Tewksbury, MA, USA). Protease inhibitor tablets, fetal bovine serum (FBS), alpha minimum essential medium (α-MEM), Dulbecco's modified Eagle medium (DMEM), horseradish peroxidase-conjugated secondary antibodies, SuperSignal West Pico Substrate, and CL-XPosure Film were purchased from Thermo Fisher Scientific (Waltham, MA, USA). Penicillin, streptomycin, 4′,6-diamidino-2-phenylindole (DAPI), and TRIzol® reagent were purchased from Invitrogen (Carlsbad, CA, USA). Melatonin, luzindole,

sirtinol, H_2O_2, propidium iodide (PI), RNase A, dexamethasone, L-ascorbic acid, β-glycerophosphate, and fluorescein diacetate (FDA) were obtained from Sigma-Aldrich (St. Louis, MO, USA). Stock solution of melatonin was prepared by dissolving in ethanol to the concentration of 200 mM, and diluting in α-MEM to different concentrations as specified in individual experiments. Primary antibodies against $p16^{INK4α}$, SIRT1, p38, p38 (phospho T180 + Y182), and α-tubulin were purchased from Abcam (Cambridge, MA, USA).

Cell culture and H_2O_2 treatment

BM-MSCs were cultured in growth medium (α-MEM supplemented with 10% FBS, 100 U/mL of penicillin, and 100 μg/mL of streptomycin) at 37°C with 5% CO_2 in 175 cm^2 cell culture flasks. The medium was changed every 3 days. Cells were dissociated by 0.25% trypsin-EDTA (Invitrogen) and reseeded into multi-well plates for the next stage of the experiments.

For induction of premature senescence, BM-MSCs at approximately 50% confluence were exposed to 100 μM, 200 μM, and 400 μM of H_2O_2 (diluted in growth medium) for 2 h. The cells were washed twice with serum-free α-MEM to remove the residual H_2O_2, re-cultured in fresh growth medium, and subjected to the subsequent tests for various durations as specified in individual experiments.

Treatments with melatonin and antagonists

The study design is depicted diagrammatically in Fig. 1. For the experiment on H_2O_2-induced premature senescence, BM-MSCs were treated with H_2O_2 at concentrations ranging from 100 μM to 400 μM for 2 h, as described above and, after washing, the cells were cultured in growth medium for an additional 4 days for subsequent experiments (Fig. 1A). For the experiment investigating the effects of melatonin pretreatment on preventing cellular senescence, BM-MSCs were pretreated with 10 nM, 1 μM, and 100 μM melatonin for 2 h followed by co-exposure to 200 μM H_2O_2 and melatonin for 2 h. After washing, the cells were incubated in growth medium without melatonin for an additional 4 days (Fig. 1B). For the experiment investigating the effects of melatonin on reversing premature senescence, BM-MSCs were treated with 200 μM H_2O_2, as stated above and, after washing, the cells were cultured in growth medium and supplemented with 10 nM, 1 μM, and 100 μM melatonin for an additional 4 days (Fig. 1C). In the osteogenic differentiation assay, BM-MSCs were treated with 200 μM H_2O_2, as described above, followed by incubation in osteogenic differentiation medium supplemented with 10 nM, 1 μM, and 100 μM melatonin for an additional 21 days (Fig. 1D). For the antagonist studies, after treating with 200 μM H_2O_2, 10 μM luzindole (a melatonin receptor inhibitor) or 40 μM sirtinol (a SIRT1 inhibitor) was added in combination with 100 μM melatonin for an additional 4 days (Fig. 1E). Luzindole and sirtinol were dissolved in DMSO and further diluted in growth medium. Cells left untreated in growth or osteogenic medium served as controls.

Cell viability assay by FDA staining

BM-MSCs were washed with phosphate buffered saline (PBS) and incubated in 5 μg/mL of FDA solution at 37°C for 10 min. The cells were washed with PBS twice and fluorescence

images were captured with an Olympus IX51 microscope (Olympus Corporation, Tokyo, Japan).

Cell proliferation assay

Cell proliferation was evaluated using the Cell Counting Kit-8 (CCK-8; Beyotime Institute of Biotechnology, Haimen, China). Ten μL of the CCK-8 solution was added to each well of 96-well plates and cells were incubated at 37°C for 1 h. Absorbance was determined at 450 nm using a microplate spectrophotometer (BioTek, Winooski, VT, USA).

SA-β-gal staining

The positive blue staining of SA-β-gal has been used as a typical biomarker of premature senescence [15]. SA-β-gal staining was performed using an SA-β-gal staining kit (Cell Signaling Technology, Beverly, MA, USA) according to the manufacturer's instructions. The cells were incubated overnight at 37°C without CO_2 and nuclei were counterstained with DAPI. To quantify the percentage of SA-β-gal-positive cells, digital images in 10 randomly chosen fields were captured by an Olympus IX51 microscope and a total of at least 200 cells from each sample were counted to calculate the percentage of senescent cells.

Cell cycle analysis

Cell cycle distribution analysis was assessed by PI staining. Adherent cells were dissociated by trypsinization and detached cells were fixed in 70% ethanol at 4°C for 24 h. After washing with PBS, samples were stained with 50 μg/mL PI and 50 μg/mL RNase A at 37°C for 30 min. Samples were analyzed using a Cytomics FC500 Flow Cytometer (Beckman-Coulter, Brea, CA, USA) and at least 5,000 cells were collected per sample. Data were analyzed using the WinMDI (Windows Multiple Document Interface for Flow Cytometry) 2.9 software.

Osteogenic differentiation and Alizarin Red S staining

BM-MSCs were first induced into premature senescence by treating with 200 μM H_2O_2. For induction of osteoblast lineage, growth medium was changed to osteogenic differentiation medium (DMEM supplemented with 10% FBS, 100 U/mL of penicillin, 100 μg/mL of streptomycin, 0.2 mM L-ascorbic acid, 100 nM dexamethasone, and 10 mM β-glycerophosphate) for 21 days in combination with 10 nM, 1 μM, and 100 μM melatonin. The medium was changed every 3 days.

Mineralization of the extracellular matrix (ECM) (a differentiation marker) was assessed by staining with 0.5% Alizarin Red S solution (Sigma-Aldrich). To quantify the calcium deposition, stained cultures were incubated in 200 μL of 1% hydrochloric acid (Sigma-Aldrich) to extract calcium-bound Alizarin Red. Absorbance of the extracted stain was measured at 420 nm using a microplate reader (BioTek).

Total RNA extraction and real-time reverse transcription-polymerase chain reaction (real-time RT-PCR)

Total RNA was extracted from the indicated cells by using TRIzol® reagent; 1 μg of total RNA was reverse-transcribed using a RevertAid First Strand cDNA Synthesis Kit (Thermo

Fisher Scientific). To quantify mRNA expression, an amount of cDNA equivalent to 20 ng of total RNA was amplified using the iTap™ Universal SYBR® Green Supermix kit (Bio-Rad, Hercules, CA, USA) on a CFX96™ Real-Time PCR System (Bio-Rad) following the manufacturer's protocol. Transcript levels of *P16INK4A*, *SIRT1*, and osteogenic marker genes, including *COL1A1* (type I collagen α1), *RUNX2* (runt-related transcription factor 2), *SPP1* (secreted phosphoprotein 1 or osteopontin), and *BGLAP*, (bone gamma carboxyglutamate protein or osteocalcin) were evaluated. *GAPDH* (glyceraldehyde-3-phosphate dehydrogenase) served as an internal standard. The primer sequences were listed in Table 1. Relative transcript levels were calculated as $\chi = 2^{-\Delta\Delta Ct}$, in which $\Delta\Delta Ct = \Delta E - \Delta C$, $\Delta E = Ct_{exp} - Ct_{GAPDH}$, and $\Delta C = Ct_{ct1} - Ct_{GAPDH}$.

Immunofluorescence staining

Cells were fixed in 4% paraformaldehyde (Sigma-Aldrich) for 15 min, blocked in 1% bovine serum albumin, and incubated in appropriately diluted primary antibodies against $p16^{INK4\alpha}$ (1:200) or SIRT1 (1:400). After rinsing with PBS, the cells were incubated in secondary antibodies (Alexa Fluor® 488 donkey anti-mouse IgG [H+L], Invitrogen, 1:1,000) and the cell nuclei were counterstained with DAPI. Fluorescence images were obtained with an Olympus IX51 microscope.

Western blot analysis

Cells were lysed in ice-cold cell lysis buffer (Beyotime) containing protease inhibitors and the protein concentration in cell extracts was quantified using the BCA protein assay kit (Beyotime). Equal amounts of protein from each extract were denatured and run in a 10% polyacrylamide gel, and then transferred by electrophoresis onto a nitrocellulose membrane (Thermo Fisher Scientific). The membrane was incubated in diluted primary antibodies at 4°C overnight. Membranes were then incubated in horseradish peroxidase-conjugated goat anti-mouse or anti-rabbit secondary antibodies. The membranes were developed using SuperSignal West Pico Substrate and CL-XPosure Film. The intensity of bands was quantified using ImageJ software (National Institutes of Health, Bethesda, MD, USA).

Statistical analysis

All data were expressed as the mean ± standard error (S.E.). Statistical differences between two groups were determined by one-way analysis of variance (ANOVA) followed by the Student's unpaired *t*-test, using the SPSS 13.0 statistical software (SPSS Inc, Chicago, IL, USA). Significance was indicated by a *p*-value of < 0.05 (*).

Results

Initially, in order to determine the effect of oxidative stress on cellular senescence, we treated BM-MSCs with 0 μM (control), 100 μM, 200 μM, and 400 μM H_2O_2 for 2 h. After 4 days, BMSCs treated with low doses of H_2O_2 (100 μM and 200 μM) showed a fibroblastic morphology but less cell density compared with untreated cells. Moreover, after treatment with 400 μM H_2O_2, cells started to float or cellular residue was found on the culture surface, indicating cell death (Fig. 2A). The CCK-8 assay confirmed that H_2O_2 exposure reduced cell growth of BM-MSCs (74.0 ± 8.1% in the 100 μM group, 28.9 ± 10.4% in the 200 μM

group, and 14.0 ± 5.5% in the 400 μM group, compared with the control) (Fig. 2B). Next, we used SA-β-gal staining to label prematurely senescent BM-MSCs; a significant increase of SA-β-gal-positive cells was observed in the H_2O_2-treated groups. In the control cells, only 9.3 ± 1.9% cells were positive for SA-β-gal staining but, after treatment with H_2O_2, the percentage of SA-β-gal-positive cells increased to 63.5 ± 5.8% at 100 μM, 86.4 ± 5.4% at 200 μM, and 93.4 ± 7.3% at 400 μM (Fig. 2C). Furthermore, the cell cycle phase distribution was examined. Cells treated with 100 μM and 200 μM H_2O_2 exhibited a significantly increased proportion in the G0/G1 phase (by 11.1% and 11.9% in comparison to the control, respectively). Meanwhile, H_2O_2-treated cells showed a lower percentage in the S phase (10.2 ± 0.9% in control cells, 3.5 ± 1.3% at 100 μM, and 3.7 ± 0.2% at 200 μM) (Fig. 2D). Cells treated with 400 μM H_2O_2 could not be collected in sufficient amounts for flow cytometry experiments. Together, the data obtained suggested that a sublethal concentration of H_2O_2 at 200 μM caused premature senescence in BM-MSCs and could be used in the subsequent experiments.

Next, we examined the preventive effect of melatonin on cellular senescence of BM-MSCs induced by 200 μM H_2O_2. BM-MSCs were pretreated with 10 nM, 1 μM, and 100 μM melatonin for 2 h and co-exposed to H_2O_2 and melatonin. The cells were then cultured for an additional 4 days without melatonin supplementation. Representative cell images showed that melatonin pretreatment did not affect cell density (Fig. 3A) and the CCK-8 assay confirmed that cell proliferation was not improved in melatonin-treated cells (Fig. 3B). The percentage of SA-β-gal-positive cells remained at a high level even after pretreatment with melatonin (88.6 ± 3.4% at 10 nM, 85.4 ± 2.4% at 1 μM, and 79.7 ± 3.3% at 100 μM) (Fig. 3C). Flow cytometry analysis revealed that pretreatment with melatonin did not change the cell cycle phase distribution. BM-MSCs pretreated with or without melatonin showed a significantly higher percentage in the G0/G1 phase and a lower proportion in the S phase than control cells (Fig. 3D). Furthermore, we examined mRNA levels of *P16INK4A* (a senescence-associated cell cycle inhibitor) and *SIRT1* (a nicotinamide adenine dinucleotide-dependent deacetylase with anti-aging abilities) in prematurely senescent BM-MSCs. Exposure to 200 μM H_2O_2 induced a 1.8 ± 0.3-fold increase of *P16INK4A* compared with the control; pretreatment with melatonin (1 μM and 100 μM) did not significantly decrease *P16INK4A* expression (Fig. 3E). The level of *SIRT1* in the H_2O_2 group was significantly lower than the control group; however, pretreatment with 1 μM and 100 μM melatonin upregulated *SIRT1* mRNA levels (Fig. 3F).

In order to further determine whether melatonin could reverse H_2O_2-induced senescence in BM-MSCs, we treated cells with 200 μM H_2O_2 and then cultured the cells supplemented with 1 nM, 1 μM, and 100 μM melatonin. Bright field and FDA-stained fluorescence images indicated increased cell density in response to melatonin (Fig. 4A). The quantitative CCK-8 assay confirmed that the cell proliferation of melatonin-treated BM-MSCs was 3.4 ± 0.2 fold at 10 nM, 4.0 ± 0.3 fold at 1 μM, and 4.3 ± 0.4 fold at 100 μM, as that of the H_2O_2-treated cells (Fig. 4B). The percentage of SA-β-gal-positive cells showed a declining dose-dependent tendency in response to melatonin, in which the ratio decreased to 64.7 ± 3.2% at 10 nM, 54.4 ± 2.3% at 1 μM, and 24.3 ± 5.7% at 100 μM (Fig. 4C). The cell cycle distribution results showed that melatonin-treated BM-MSCs exhibited a significantly

increased proportion in the S phase (5.9 ± 0.8% at 10 nM, 6.4 ± 0.8% at 1 μM, and 7.8 ± 0.3% at 100 μM) (Fig. 4D). Treatment with 100 μM melatonin significantly decreased H_2O_2-stimulated expression of *P16INK4A* by 40.9% compared with the H_2O_2-treated cells (Fig. 4E). On the other hand, treatment with 100 μM melatonin increased the *SIRT1* mRNA level by 1.8 ± 0.2-fold higher than the H_2O_2 group (Fig. 4F).

An important parameter for defining MSCs is their multipotent differentiation; here, we analyzed whether the *in vitro* osteogenic potential of BM-MSCs was affected by H_2O_2-induced premature senescence or recovered with supplementation with melatonin. Mineralization of the ECM demonstrated, upon staining with Alizarin Red S dye, that H_2O_2-induced premature senescence inhibited the differentiation of BM-MSCs into the osteoblast lineage (17.9 ± 2.4% in contrast with the control). However, mineralized areas in melatonin-treated cells showed a dose-dependent increase; treatment with 100 μM melatonin increased the mineralization level by 2.9 ± 0.4-fold compared with the H_2O_2-treated cells (Fig. 5A). To evaluate the propensity for osteogenic differentiation, transcript levels of osteoblast-specific genes were examined. Exposure to H_2O_2 reduced *COL1A1* expression by 50.3 ± 1.2% compared with the control. In contrast, supplementation with melatonin significantly upregulated the *COL1A1* mRNA levels by 59.1 ± 7.6% at 10 nM, 73.1 ± 7.5% at 1 μM, and 88.9 ± 18.4% at 100 μM, compared to the H_2O_2-treated cells (Fig. 5B). The transcription factor RUNX2, which plays a critical role in MSC osteogenesis, decreased to 18.4 ± 1.9% after H_2O_2 exposure, but treatment with melatonin increased the mRNA levels by 1.7 ± 0.2-fold, 2.8 ± 0.2-fold, and 3.0 ± 0.2-fold at concentrations ranging from 1 nM to 100 μM, respectively (Fig. 5C). Similarly, treatment with 100 μM melatonin elevated the mRNA levels of *SPP1* by 66.7 ± 14.2% (Fig. 5D) and *BGLAP* by 4.5 ± 0.5-fold (Fig. 5E), compared to the H_2O_2-treated cells. These results suggest that treatment with melatonin enhanced the osteogenic differentiation of senescent BM-MSCs.

Previous studies reported that the accumulation of $p16^{INK4\alpha}$ led to induction of cellular senescence through the p38 MAPK signaling pathway [33]. Therefore, we hypothesized that $p16^{INK4\alpha}$ could be the target of melatonin. Immunofluorescence staining revealed that the expression of $p16^{INK4\alpha}$ was suppressed by treatment with melatonin in H_2O_2-induced senescent BM-MSCs. In contrast, exposure to H_2O_2 inhibited SIRT1 protein expression but treatment with melatonin recovered it (Fig. 6A). Western blot analysis confirmed that H_2O_2 exposure enhanced $p16^{INK4\alpha}$ protein levels by 8.5 ± 0.7-fold compared with the control, whereas treatment with melatonin attenuated $p16^{INK4\alpha}$ expression by 47.0 ± 5.7% compared with the H_2O_2 group (Fig. 6B). Further experiments revealed that the protein level of SIRT1 in H_2O_2-treated BM-MSCs was significantly down-regulated to 42.8 ± 6.3% compared with the control, but treatment with melatonin upregulated the level of SIRT1 (Fig. 6C). To determine the role of p38 in H_2O_2-induced premature senescence, we detected the levels of phosphorylation (p-) and total p38. The western blot assays showed that exposure to H_2O_2 enhanced phosphorylation of p38 by 4.5 ± 0.6-fold compared with the control, whereas treatment with melatonin attenuated p-p38 expression by 64.0 ± 5.3% compared with the H_2O_2 group. However, we found that total p38 protein expression did not vary in all groups (Fig. 6D).

Luzindole, a nonselective antagonist of melatonin receptors, was used to determine whether the effects of melatonin on H_2O_2-induced premature senescence were mediated through the melatonin receptor pathway. Supplementation with luzindole inhibited the protective effects of melatonin by elevating the percentage of SA-β-gal-positive BM-MSCs to 68.6 ± 5.9% (Fig. 7A). Although treatment with luzindole reversed the suppressive effects of melatonin on *P16INK4A* mRNA expression, the difference was not significant ($p = 0.20$) (Fig. 7B). In contrast, *SIRT1* mRNA levels were significantly lower in the H_2O_2+MT+Luz group by 55.7 ± 2.0% than the H_2O_2+MT group (Fig. 7C). The western blot results were consistent with the real-time RT-PCR data, in which SIRT1 protein expression was 61.7 ± 6.7% lower after treatment with luzindole compared to the H_2O_2+MT group (Fig. 7D).

To further determine the involvement of SIRT1 in modulating melatonin-mediated anti-senescence effects, we used sirtinol to specifically inhibit SIRT1 activity. Using sirtinol treatment alone, the percentage of SA-β-gal-positive BM-MSCs increased to 41.3 ± 4.6% compared to 9.0 ± 2.5% in the control. Supplementation with sirtinol significantly blocked the melatonin-mediated anti-senescence effects by raising the percentage of SA-β-gal-positive cells to 89.8 ± 4.4% (Fig. 8A). Treatment with sirtinol upregulated *P16INK4A* mRNA levels ($p = 0.37$) (Fig. 8B) and down-regulated *SIRT1* ($p = 0.03$) (Fig. 8C), compared with the H_2O_2+MT group. The western blot assay showed that $p16^{INK4\alpha}$ protein levels were significantly (1.2-fold) higher after treatment with sirtinol compared with the H_2O_2+MT group. In contrast, SIRT1 protein levels were significantly (48.1 ± 8.4%) lower after treatment with sirtinol than the H_2O_2+MT group (Fig. 8D).

Discussion

In the present study, we examined the effects and underlying mechanisms of melatonin on H_2O_2-induced premature senescence in human BM-MSCs. Our results demonstrated that treatment with melatonin reverses cellular senescence in a dose-dependent manner and that melatonin-mediated anti-senescence effects involve activation of the SIRT1 pathway.

Herein, to avoid replicative senescence induced by contact inhibition [34] or over-proliferation [35], we cultured BM-MSCs to approximately 50% cell density, followed by H_2O_2 or melatonin treatment. Furthermore, transplantation of MSCs to repair damaged tissues or organs is promising in regenerative medicine, but pathological conditions, such as an inflammatory environment with abnormal levels of oxidative stress, compromise the regenerative abilities of MSCs by inducing the cells into senescence or apoptosis. Previous studies showed that exposure to high concentrations of H_2O_2 damaged cell survival by increasing DNA fragmentation and the Bax/Bcl-2 ratio [36]. In the current study, we tested the effects of a serial concentration of H_2O_2 on MSC senescence. Our results showed that low-moderate concentrations of H_2O_2, such as 100 μM and 200 μM, induced positive staining of SA-β-gal activity and arrested cell cycle progression, but a high dose of H_2O_2 at 400 μM resulted in cell death, in agreement with a recent report [37]. Thus, we used a 200 μM concentration H_2O_2 treatment in the rest of our experiments.

The cytoprotective effects of melatonin on MSCs and other types of cells from oxidative stress have been studied extensively. Wang et al. [38] reported that pretreatment with

melatonin attenuated H_2O_2-induced MSC apoptosis by suppressing intracellular ROS generation and inhibiting caspase-3 activation. In a murine senescence model, treatment with melatonin improved pro-survival processes by increasing expression of anti-apoptotic proteins such as Bcl-2_{XL} [39]. Exogenous supplementation with melatonin counteracted the pro-apoptotic effects of proinflammatory cytokines through attenuation of intracellular ROS accumulation [27]. Nevertheless, the influence and underlying mechanisms of melatonin on H_2O_2–induced premature senescence of MSCs were not elucidated in previous studies. Our present results showed that exogenous supplementation with melatonin successfully protected MSCs from H_2O_2–induced senescence in a dose-dependent manner, as evidenced by a decreased percentage of SA-β-gal-positive cells, increased cell proliferative potential, and suppressed levels of $p16^{INK4\alpha}$. Also, some antioxidant drugs showed similar anti-senescence effects. For instance, exogenously added resveratrol attenuated oxidative stress-induced aging and improved cell proliferation in endothelial cells [40]. These findings provide experimental strategies for utilization of MSC-based cell therapy with defense against oxidative damage.

The most important findings in our present study were that treatment with melatonin after exposure to H_2O_2 attenuated the senescent phenotypes of BM-MSCs, whereas pretreatment with melatonin failed to prevent oxidative stress-induced premature senescence. Excessive levels of H_2O_2 are deleterious to MSCs by causing increased DNA damage and inhibiting DNA synthesis and cell proliferation. This damage resulted in the activation of cell cycle checkpoint proteins (e.g. $p16^{INK4\alpha}$) and initiation of the process of DNA repair. During the recovery time, the unrepaired, damaged DNA in the MSCs led to premature senescence and ultimately cell apoptosis or death. In our study, treatment with melatonin was applied before and during the exposure to H_2O_2 for 2 h. Melatonin was able to enhance the intracellular antioxidant defense by increasing expression of catalase and glutathione peroxidase [41], but it could not directly eliminate exogenously added H_2O_2. In addition, MSCs were pre-incubated with melatonin for only 2 h; we speculated that the period of pretreatment with melatonin may not be long enough to prevent DNA damage and subsequent prematurely senescent phenotypes. On the other hand, treatment with melatonin after exposure to H_2O_2 may contribute to DNA repair [42], inhibit the p38-$p16^{INK4\alpha}$ signaling pathway, and finally reverse H_2O_2–induced premature senescence. Therefore, we will use melatonin as a supplement for MSC *in vitro* expansion, and examine the long-term effects of melatonin on oxidative stress-induced or replicative senescence of MSCs. Moreover, our results demonstrated that luzindole, an inhibitor of melatonin receptors, counteracted the melatonin-mediated anti-senescence effects on H_2O_2-treated BM-MSCs. Consistent with previous studies [26, 43], the present findings suggest that the anti-senescence effects of melatonin on MSCs were mediated, at least in part, through activation of melatonin receptor-related signaling pathways.

Cell cycle arrest by increased expression of CKI, such as $p16^{INK4\alpha}$, is a hallmark of cellular senescence of MSCs [44]. The protein $p16^{INK4\alpha}$, as an inhibitor for the cell cycle kinases CDK4 and CDK6, was found to be accumulated in aged and oxidative stress-induced cells [45]. The observation of increased ratios of cells subjected to H_2O_2 in the G0/G1 phase is in agreement with a previous report of normal human epidermal keratinocytes exposed to

oxidative stress [46]. Treatment with melatonin dose-dependently improved the entry of proliferating cells into the S phase and decreased $p16^{INK4\alpha}$ expression compared with H_2O_2-treated BM-MSCs. However, the percentage of melatonin-treated cells in the G0/G1 phase did not decrease significantly, indicating exposure to H_2O_2 possibly induced MSCs into G2 cell cycle arrest [47]; thus, we will investigate the effects of melatonin on cell cycle-related proteins in MSCs in future studies.

The regenerative potential of MSCs is essential for their therapeutic application; hence, we tested the impacts of H_2O_2 and melatonin on the propensity for osteogenic differentiation. Prematurely senescent MSCs exhibited an impaired osteogenic potential, as evidenced by weak staining for mineralized ECM and suppressed levels of osteoblast-specific genes. Consistent with our results, Ho et al. [14] showed that H_2O_2 accumulation in MSCs resulted not only in cellular senescence but also in the decline of osteogenic differentiation. Therefore, targeting excessive levels of oxidative stress associated with senescence may improve multilineage differentiation capacity and benefit the clinical utilization of MSCs [48, 49]. On the other hand, it has been recently reported that MSCs with replicative senescence showed reduced adipogenic differentiation and enhanced osteogenic differentiation, possibly due to decreased levels of PPARγ that shifted the balance of adipogenic and osteogenic lineage commitment of MSCs [17]. The conflicting findings suggested that premature or replicatively senescent MSCs may have intrinsically different gene profiles and signaling pathways to direct their lineage-specific commitment. In addition, melatonin improved osteogenic differentiation of senescent BM-MSCs because of attenuation of ROS [26] and activation of the MAPK-ERK (extracellular signal-regulated kinases) signaling cascade [50]. More importantly, extensive studies have shown that age-related senescence in bone marrow-derived MSCs (BM-MSCs) leads to the impairment of their regenerative potentials. In accordance, a significant decline in endogenous melatonin levels during physiological and pathological aging has been reported. Magri et al. [51] demonstrated that plasma melatonin levels are significantly lower in older people than in young individuals. Therefore, we speculated that the reduction of melatonin levels with age is associated with the increased senescence of BM-MSCs and our future work will focus on the effects of melatonin on aged cells and tissue repair.

In the search for the molecular mechanisms involved in melatonin-mediated anti-senescence effects, p38 activation was found in H_2O_2-treated BM-MSCs in this study. Borodkina et al. [52] observed an increased phosphorylation level of p38 that was suggested to contribute to H_2O_2-induced senescence of MSCs, because the pharmacological inhibition of p38 sufficiently recovered cells from senescent phenotypes. We found that premature senescence of BM-MSCs was associated with upregulated $p16^{INK4\alpha}$ expression, which was reported at a high level in aging individuals and was responsible for age-dependent cellular senescence [53]. In addition, the decline of SIRT1 expression was observed in H_2O_2-treated BM-MSCs with premature senescence. An *in vitro* study on senescent endothelial progenitor cells showed that downregulation of SIRT1 positively correlated to accelerated senescence and dysfunctional angiogenic activity [54]. Our results demonstrated that melatonin reversed H_2O_2-induced prematurely senescent BM-MSCs in the SIRT1-dependent manner because the pharmacological inhibition of SIRT1 by sirtinol abrogated the protective effects of

melatonin. Together with other previous reports [55], the data suggest that melatonin reversed premature senescence of MSCs and decreased $p16^{INK4\alpha}$ expression through the SIRT1-dependent pathway. Furthermore, activation of the p53/p21 pathway is another important mechanism involved in the induction of cellular senescence. Increased p53 acetylation was found in senescent cells accompanied with reduction of SIRT1 levels; p53 promotes the transcription of p21, which is a critical cell cycle controller. Both inhibition of p53 and activation of SIRT1 by resveratrol could prevent glucocorticoid-induced senescence in primary tenocytes [56]. Thus, further work is necessary to elucidate the underlying mechanisms by which melatonin modulates the p53/p21 signaling pathway in senescent MSCs induced by oxidative stress.

In conclusion, our work identifies melatonin as a strong candidate for incorporation into new anti-senescence strategies in an effort to protect MSCs from H_2O_2-induced premature senescence. Treatment with melatonin effectively reversed senescent phenotypes by decreasing the percentage of SA-β-gal-positive cells, increasing cell proliferation, promoting the entry of cells into the S phase, and restoring osteogenic differentiation potentials of BM-MSCs in a dose-dependent manner. The protective effects are associated with the downregulation of $p16^{INK4\alpha}$ expression and upregulation of SIRT1 levels through melatonin membrane receptor-dependent pathways. Our findings lay the groundwork for understanding oxidative stress-induced premature senescence and promoting therapeutic utilization of melatonin in stem cell-based regenerative medicine.

Acknowledgments

The authors are grateful to Suzanne Danley (West Virginia University, USA), Michelle Si (University of Waterloo, Canada), and Joseph Jargstorf (University of Waterloo, Canada) for carefully reviewing and editing the manuscript. This work was supported by the National Natural Science Foundation of China (No.51203194, No.51103182, No. 21204056, No.31270995, No.81320108018); the National Institutes of Health (NIH) (R03 AR062763-01A1); Natural Science Foundation of Jiangsu Province (No.BK20140323, No.BK2012173); Jiangsu Provincial Special Program of Medical Science (BL2012004); Jiangsu Provincial Clinical Orthopedic Center; the Priority Academic Program Development of Jiangsu Higher Education Institutions (PAPD); Scientific Research Foundation for the Returned Overseas Chinese Scholars, State Education Ministry; Science and Technology Program of Guangzhou [2013] 164, China.

References

1. PITTENGER MF, MACKAY AM, BECK SC, et al. Multilineage potential of adult human mesenchymal stem cells. Science. 1999; 284:143–147. [PubMed: 10102814]
2. OREFFO RO, COOPER C, MASON C, et al. Mesenchymal stem cells: lineage, plasticity, and skeletal therapeutic potential. Stem Cell Rev. 2005; 1:169–178. [PubMed: 17142852]
3. VIDAL MA, WALKER NJ, NAPOLI E, et al. Evaluation of senescence in mesenchymal stem cells isolated from equine bone marrow, adipose tissue, and umbilical cord tissue. Stem Cells Dev. 2012; 21:273–283. [PubMed: 21410356]
4. BRANDL A, MEYER M, BECHMANN V, et al. Oxidative stress induces senescence in human mesenchymal stem cells. Exp Cell Res. 2011; 317:1541–1547. [PubMed: 21376036]
5. DUMONT P, BURTON M, CHEN QM, et al. Induction of replicative senescence biomarkers by sublethal oxidative stresses in normal human fibroblast. Free Radic Biol Med. 2000; 28:361–373. [PubMed: 10699747]
6. VACANTI V, KONG E, SUZUKI G, et al. Phenotypic changes of adult porcine mesenchymal stem cells induced by prolonged passaging in culture. J Cell Physiol. 2005; 205:194–201. [PubMed: 15880640]

7. MEZEY E. The therapeutic potential of bone marrow-derived stromal cells. J Cell Biochem. 2011; 112:2683–2687. [PubMed: 21678464]
8. HE H, LIU X, PENG L, et al. Promotion of hepatic differentiation of bone marrow mesenchymal stem cells on decellularized cell-deposited extracellular matrix. Biomed Res Int. 2013; 2013:406871. [PubMed: 23991414]
9. KASSEM M, MARIE PJ. Senescence-associated intrinsic mechanisms of osteoblast dysfunctions. Aging cell. 2011; 10:191–197. [PubMed: 21210937]
10. LI J, PEI M. Cell senescence: a challenge in cartilage engineering and regeneration. Tissue Eng Part B Rev. 2012; 18:270–287. [PubMed: 22273114]
11. KSIAZEK K. A comprehensive review on mesenchymal stem cell growth and senescence. Rejuvenation Res. 2009; 12:105–116. [PubMed: 19405814]
12. VAN DE BITTNER GC, DUBIKOVSKAYA EA, BERTOZZI CR, et al. In vivo imaging of hydrogen peroxide production in a murine tumor model with a chemoselective bioluminescent reporter. Proc Natl Acad Sci U S A. 2010; 107:21316–21321. [PubMed: 21115844]
13. WEI H, LI Z, HU S, et al. Apoptosis of mesenchymal stem cells induced by hydrogen peroxide concerns both endoplasmic reticulum stress and mitochondrial death pathway through regulation of caspases, p38 and JNK. J Cell Biochem. 2010; 111:967–978. [PubMed: 20665666]
14. HO PJ, YEN ML, TANG BC, et al. H2O2 accumulation mediates differentiation capacity alteration, but not proliferative decline, in senescent human fetal mesenchymal stem cells. Antioxid Redox Signal. 2013; 18:1895–1905. [PubMed: 23088254]
15. BUROVA E, BORODKINA A, SHATROVA A, et al. Sublethal oxidative stress induces the premature senescence of human mesenchymal stem cells derived from endometrium. Oxid Med Cell Longev. 2013; 2013:474931. [PubMed: 24062878]
16. MULLER M. Cellular senescence: molecular mechanisms, in vivo significance, and redox considerations. Antioxid Redox Signal. 2009; 11:59–98. [PubMed: 18976161]
17. CHENG H, QIU L, MA J, et al. Replicative senescence of human bone marrow and umbilical cord derived mesenchymal stem cells and their differentiation to adipocytes and osteoblasts. Mol Biol Rep. 2011; 38:5161–5168. [PubMed: 21188535]
18. COLLINS CJ, SEDIVY JM. Involvement of the INK4a/Arf gene locus in senescence. Aging cell. 2003; 2:145–150. [PubMed: 12882406]
19. HUANG J, GAN Q, HAN L, et al. SIRT1 overexpression antagonizes cellular senescence with activated ERK/S6k1 signaling in human diploid fibroblasts. PLoS One. 2008; 3:e1710. [PubMed: 18320031]
20. VAZIRI H, DESSAIN SK, NG EATON E, et al. hSIR2(SIRT1) functions as an NAD-dependent p53 deacetylase. Cell. 2001; 107:149–159. [PubMed: 11672523]
21. HAN L, ZHOU R, NIU J, et al. SIRT1 is regulated by a PPARγ-SIRT1 negative feedback loop associated with senescence. Nucleic Acids Res. 2010; 38:7458–7471. [PubMed: 20660480]
22. TAN DX, MANCHESTER LC, REITER RJ, et al. Identification of highly elevated levels of melatonin in bone marrow: its origin and significance. Biochim Biophys Acta. 1999; 1472:206–214. [PubMed: 10572942]
23. REITER RJ. Pineal melatonin: cell biology of its synthesis and of its physiological interactions. Endocr Rev. 1991; 12:151–180. [PubMed: 1649044]
24. GALANO A, TAN DX, REITER RJ. On the free radical scavenging activities of melatonin's metabolites, AFMK and AMK. J Pineal Res. 2013; 54:245–257. [PubMed: 22998574]
25. ZHANG HM, ZHANG Y. Melatonin: a well-documented antioxidant with conditional pro-oxidant actions. J Pineal Res. 2014; 57:131–146. [PubMed: 25060102]
26. LIU X, GONG Y, XIONG K, et al. Melatonin mediates protective effects on inflammatory response induced by interleukin-1 beta in human mesenchymal stem cells. J Pineal Res. 2013; 55:14–25. [PubMed: 23488678]
27. LIU X, XU Y, CHEN S, et al. Rescue of proinflammatory cytokine-inhibited chondrogenesis by the antiarthritic effect of melatonin in synovium mesenchymal stem cells via suppression of reactive oxygen species and matrix metalloproteinases. Free Radic Biol Med. 2014; 68:234–246. [PubMed: 24374373]

28. HE F, LIU X, XIONG K, et al. Extracellular matrix modulates the biological effects of melatonin in mesenchymal stem cells. J Endocrinol. 2014; 223:167–180. [PubMed: 25210047]
29. PEI M, HE F, WEI L, et al. Melatonin enhances cartilage matrix synthesis by porcine articular chondrocytes. J Pineal Res. 2009; 46:181–187. [PubMed: 19054299]
30. HUI JH, LI L, TEO YH, et al. Comparative study of the ability of mesenchymal stem cells derived from bone marrow, periosteum, and adipose tissue in treatment of partial growth arrest in rabbit. Tissue Eng. 2005; 11:904–912. [PubMed: 15998230]
31. YU L, SUN Y, CHENG L, et al. Melatonin receptor-mediated protection against myocardial ischemia/reperfusion injury: role of SIRT1. J Pineal Res. 2014; 57:228–238. [PubMed: 25052362]
32. PROIETTI S, CUCINA A, DOBROWOLNY G, et al. Melatonin down-regulates MDM2 gene expression and enhances p53 acetylation in MCF-7 cells. J Pineal Res. 2014; 57:120–129. [PubMed: 24920214]
33. CHANG J, LI Y, HUANG Y, et al. Adiponectin prevents diabetic premature senescence of endothelial progenitor cells and promotes endothelial repair by suppressing the p38 MAP kinase/p16INK4A signaling pathway. Diabetes. 2010; 59:2949–2459. [PubMed: 20802255]
34. HO JH, CHEN YF, MA WH, et al. Cell contact accelerates replicative senescence of human mesenchymal stem cells independent of telomere shortening and p53 activation: roles of Ras and oxidative stress. Cell Transplant. 2011; 20:1209–1220. [PubMed: 21176396]
35. WAGNER W, HORN P, CASTOLDI M, et al. Replicative senescence of mesenchymal stem cells: a continuous and organized process. PLoS One. 2008; 3:e2213. [PubMed: 18493317]
36. NIWA K, INANAMI O, YAMAMORI T, et al. Redox regulation of PI3K/Akt and p53 in bovine aortic endothelial cells exposed to hydrogen peroxide. Antioxid Redox Signal. 2003; 5:713–722. [PubMed: 14588144]
37. KO E, LEE KY, HWANG DS. Human umbilical cord blood-derived mesenchymal stem cells undergo cellular senescence in response to oxidative stress. Stem Cells Dev. 2012; 21:1877–1886. [PubMed: 22066510]
38. WANG FW, WANG Z, ZHANG YM, et al. Protective effect of melatonin on bone marrow mesenchymal stem cells against hydrogen peroxide-induced apoptosis in vitro. J Cell Biochem. 2013; 114:2346–2355. [PubMed: 23824714]
39. GUTIERREZ-CUESTA J, TAJES M, JIMENEZ A, et al. Evaluation of potential pro-survival pathways regulated by melatonin in a murine senescence model. J Pineal Res. 2008; 45:497–505. [PubMed: 18705649]
40. KAO CL, CHEN LK, CHANG YL, et al. Resveratrol protects human endothelium from H(2)O(2)-induced oxidative stress and senescence via SirT1 activation. J Atheroscler Thromb. 2010; 17:970–979. [PubMed: 20644332]
41. FISCHER TW, KLESZCZYNSKI K, HARDKOP LH, et al. Melatonin enhances antioxidative enzyme gene expression (CAT, GPx, SOD), prevents their UVR-induced depletion, and protects against the formation of DNA damage (8-hydroxy-2′-deoxyguanosine) in ex vivo human skin. J Pineal Res. 2013; 54:303–312. [PubMed: 23110400]
42. LIU R, FU A, HOFFMAN AE, et al. Melatonin enhances DNA repair capacity possibly by affecting genes involved in DNA damage responsive pathways. BMC Cell Biol. 2013; 14:1. [PubMed: 23294620]
43. TANG Y, CAI B, YUAN F, et al. Melatonin pretreatment improves the survival and function of transplanted mesenchymal stem cells after focal cerebral ischemia. Cell Transplant. 2013; 23:1279–1291. [PubMed: 25330060]
44. SERRANO M, HANNON GJ, BEACH D. A new regulatory motif in cell-cycle control causing specific inhibition of cyclin D/CDK4. Nature. 1993; 366:704–707. [PubMed: 8259215]
45. KRISHNAMURTHY J, TORRICE C, RAMSEY MR, et al. Ink4a/Arf expression is a biomarker of aging. J Clin Invest. 2004; 114:1299–1307. [PubMed: 15520862]
46. SASAKI M, KAJIYA H, OZEKI S, et al. Reactive oxygen species promotes cellular senescence in normal human epidermal keratinocytes through epigenetic regulation of p16(INK4a.). Biochem Biophys Res Commun. 2014; 452:622–628. [PubMed: 25181340]
47. LI M, ZHAO L, LIU J, et al. Hydrogen peroxide induces G2 cell cycle arrest and inhibits cell proliferation in osteoblasts. Anat Rec. 2009; 292:1107–1113.

48. CHOI YJ, LEE JY, CHUNG CP, et al. Cell-penetrating superoxide dismutase attenuates oxidative stress-induced senescence by regulating the p53-p21(Cip1) pathway and restores osteoblastic differentiation in human dental pulp stem cells. Int J Nanomed. 2012; 7:5091–5106.

49. PEI M, ZHANG Y, LI J, et al. Antioxidation of decellularized stem cell matrix promotes human synovium-derived stem cell-based chondrogenesis. Stem Cells Dev. 2013; 22:889–900. [PubMed: 23092115]

50. RADIO NM, DOCTOR JS, WITT-ENDERBY PA. Melatonin enhances alkaline phosphatase activity in differentiating human adult mesenchymal stem cells grown in osteogenic medium via MT2 melatonin receptors and the MEK/ERK (1/2) signaling cascade. J Pineal Res. 2006; 40:332–342. [PubMed: 16635021]

51. MAGRI F, SARRA S, CINCHETTI W, et al. Qualitative and quantitative changes of melatonin levels in physiological and pathological aging and in centenarians. J Pineal Res. 2004; 36:256–261. [PubMed: 15066050]

52. BORODKINA A, SHATROVA A, ABUSHIK P, et al. Interaction between ROS dependent DNA damage, mitochondria and p38 MAPK underlies senescence of human adult stem cells. Aging. 2014; 6:481–495. [PubMed: 24934860]

53. HEISS C, KEYMEL S, NIESLER U, et al. Impaired progenitor cell activity in age-related endothelial dysfunction. J Am Coll Cardiol. 2005; 45:1441–1448. [PubMed: 15862416]

54. VASSALLO PF, SIMONCINI S, LIGI I, et al. Accelerated senescence of cord blood endothelial progenitor cells in premature neonates is driven by SIRT1 decreased expression. Blood. 2014; 123:2116–2126. [PubMed: 24518759]

55. YUAN HF, ZHAI C, YAN XL, et al. SIRT1 is required for long-term growth of human mesenchymal stem cells. J Mol Med. 2012; 90:389–400. [PubMed: 22038097]

56. POULSEN RC, WATTS AC, MURPHY RJ, et al. Glucocorticoids induce senescence in primary human tenocytes by inhibition of sirtuin 1 and activation of the p53/p21 pathway: in vivo and in vitro evidence. Ann Rheum Dis. 2014; 73:1405–1413. [PubMed: 23727633]

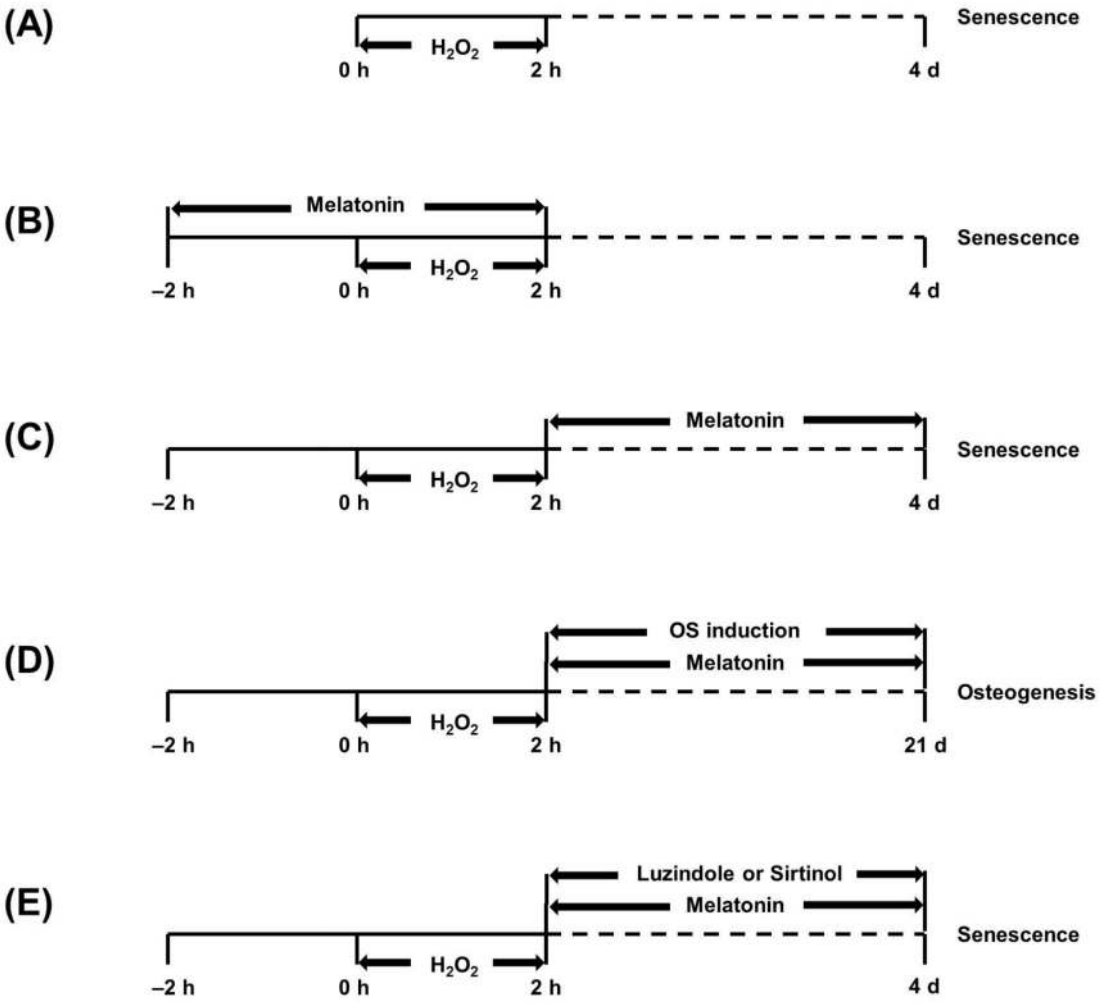

Fig. 1.

The study design for investigating the effects of melatonin on H_2O_2-induced premature senescence in BM-MSCs. (A) Exposure to H_2O_2 induced premature senescence in BM-MSCs. (B) To examine whether melatonin could prevent H_2O_2-induced premature senescence, treatment with melatonin was applied before H_2O_2 exposure. (C) To examine whether melatonin could reverse H_2O_2-induced premature senescence, treatment with melatonin was applied after H_2O_2 exposure. (D) To examine whether melatonin could restore senescence-inhibited osteogenic (OS) differentiation, treatment with melatonin was applied after H_2O_2 exposure. (E) Underlying mechanisms of melatonin-mediated anti-senescence effects were revealed by inhibition of melatonin membrane receptors by luzindole or SIRT1 by sirtinol.

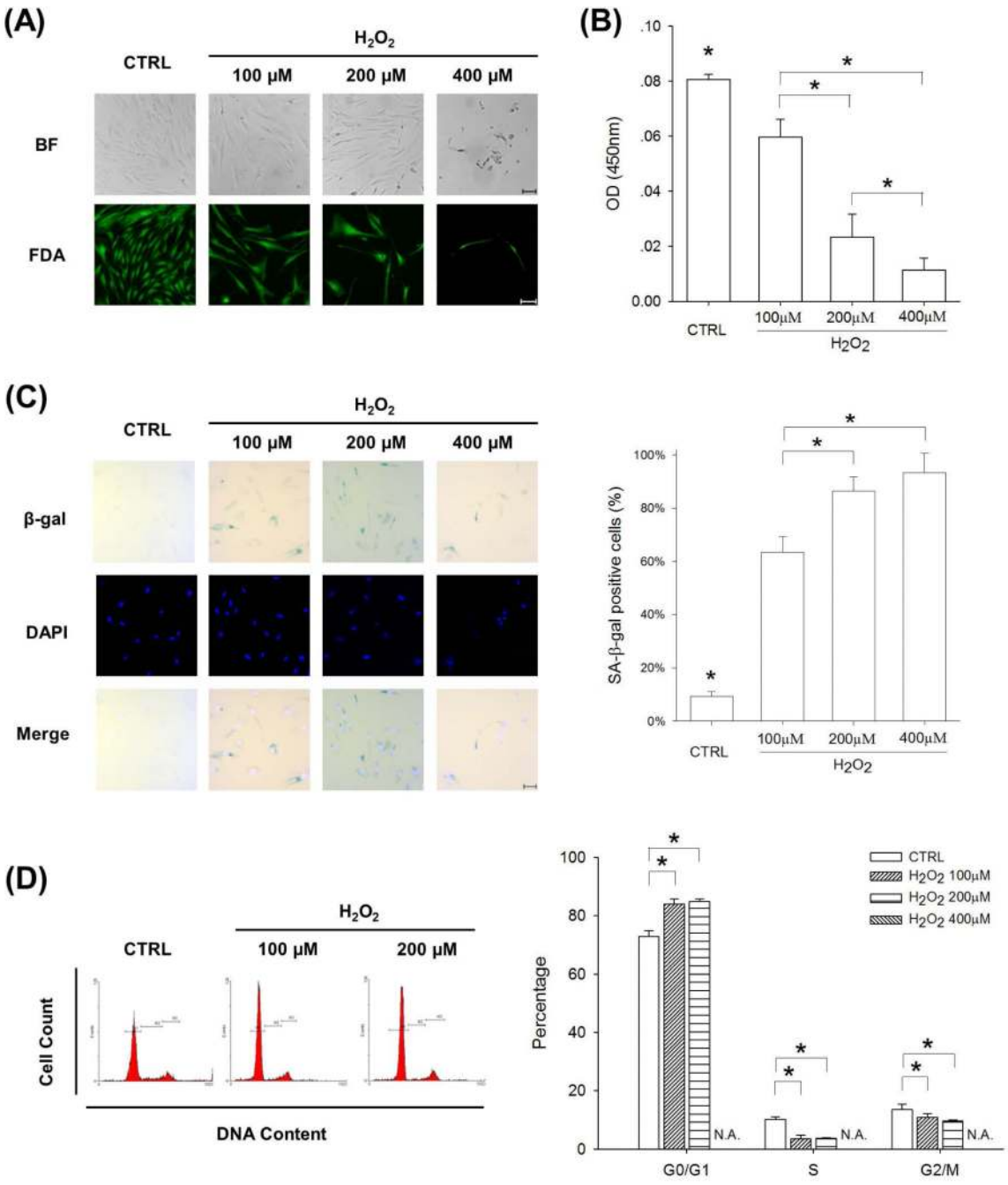

Fig. 2.

H_2O_2 treatment induced premature senescence-associated features in BM-MSCs in a dose-dependent manner. (A) Cell morphology and density were observed in representative bright field (BF) images and fluorescence images labeled by fluorescein diacetate (FDA). Scale bar = 100 μm. (B) Cell proliferation, determined by the CCK-8 assay, was suppressed by H_2O_2 treatment. Values are the mean ± S.E. of six independent experiments (n = 6). (C) BM-MSCs were stained for SA-β-gal (blue) and the nuclei were counterstained with DAPI. The percentage of SA-β-gal-positive cells showed a dose-dependent increase in response to

H_2O_2. Scale bar = 50 μm. (D) Flow cytometry analysis was used to measure the cell cycle distribution of BM-MSCs. H_2O_2 treatment induced G1 cell cycle arrest. Values are the mean ± S.E. of three independent experiments (n = 3). Statistically significant differences are indicated by * ($p < 0.05$).

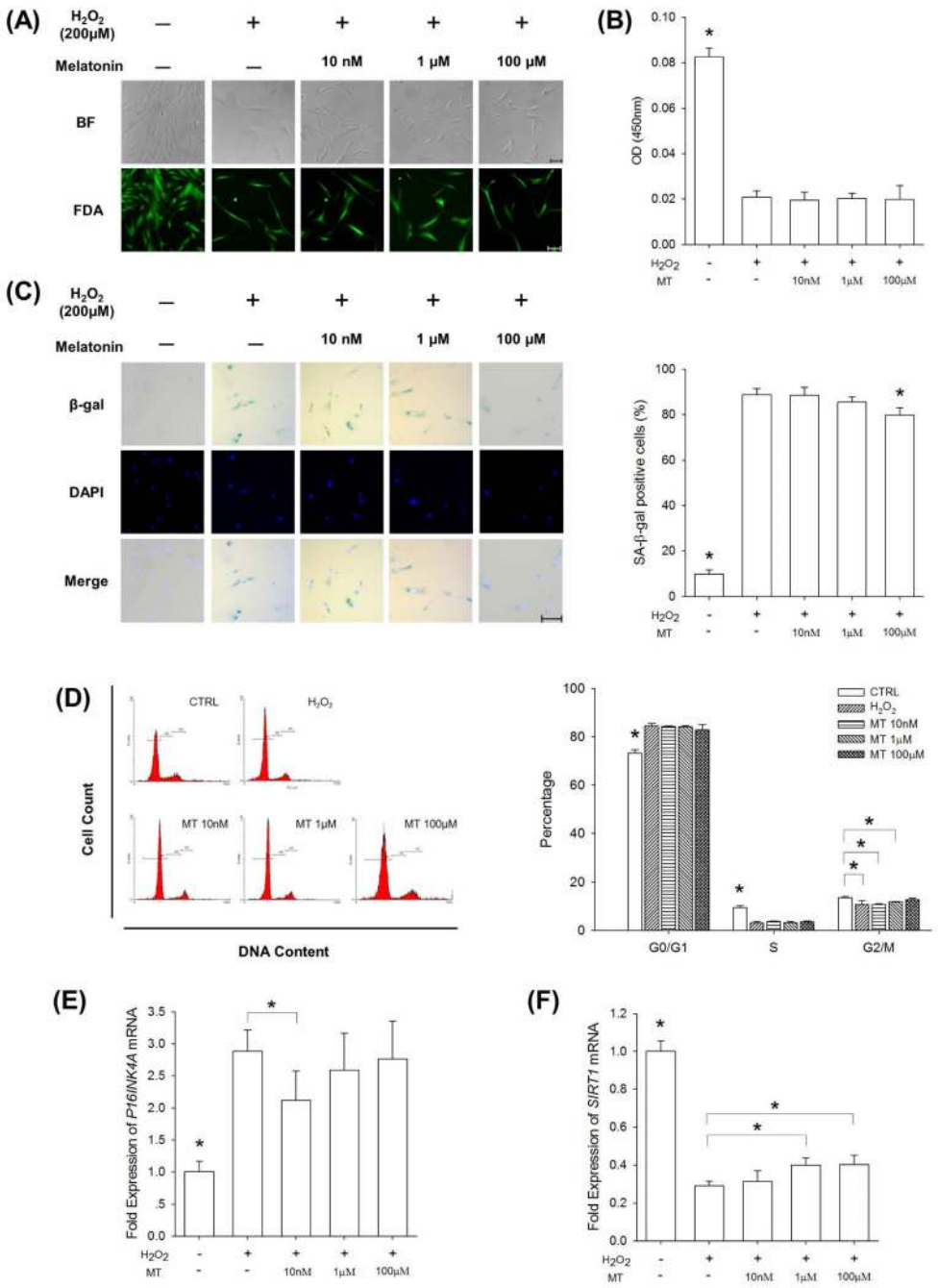

Fig. 3.

Pretreatment with melatonin cannot significantly prevent H_2O_2-induced premature senescence. BM-MSCs were pretreated with 10 nM, 1 μM, and 100 μM melatonin, and then co-exposed to 200 μM H_2O_2. (A) Cell morphology and density were observed in representative bright field (BF) images and fluorescence images labeled by fluorescein diacetate (FDA). Scale bar = 100 μm. (B) Cell proliferation was determined by the CCK-8 assay. Values are the mean ± S.E. of six independent experiments (n = 6). (C) Representative SA-β-gal (blue) staining images of BM-MSCs indicated senescent cells. The

percentage of SA-β-gal-positive cells was retained at a high level after pretreatment with melatonin. Scale bar = 50 μm. (D) Flow cytometry analysis revealed that pretreatment with melatonin did not prevent H_2O_2-induced cell cycle arrest. Values are the mean ± S.E. of three independent experiments ($n = 3$). The mRNA levels of *P16INK4A* (E) and *SIRT1* (F) were measured by real-time RT-PCR. Values are the mean ± S.E. of four independent experiments ($n = 4$). Statistically significant differences are indicated by * ($p < 0.05$).

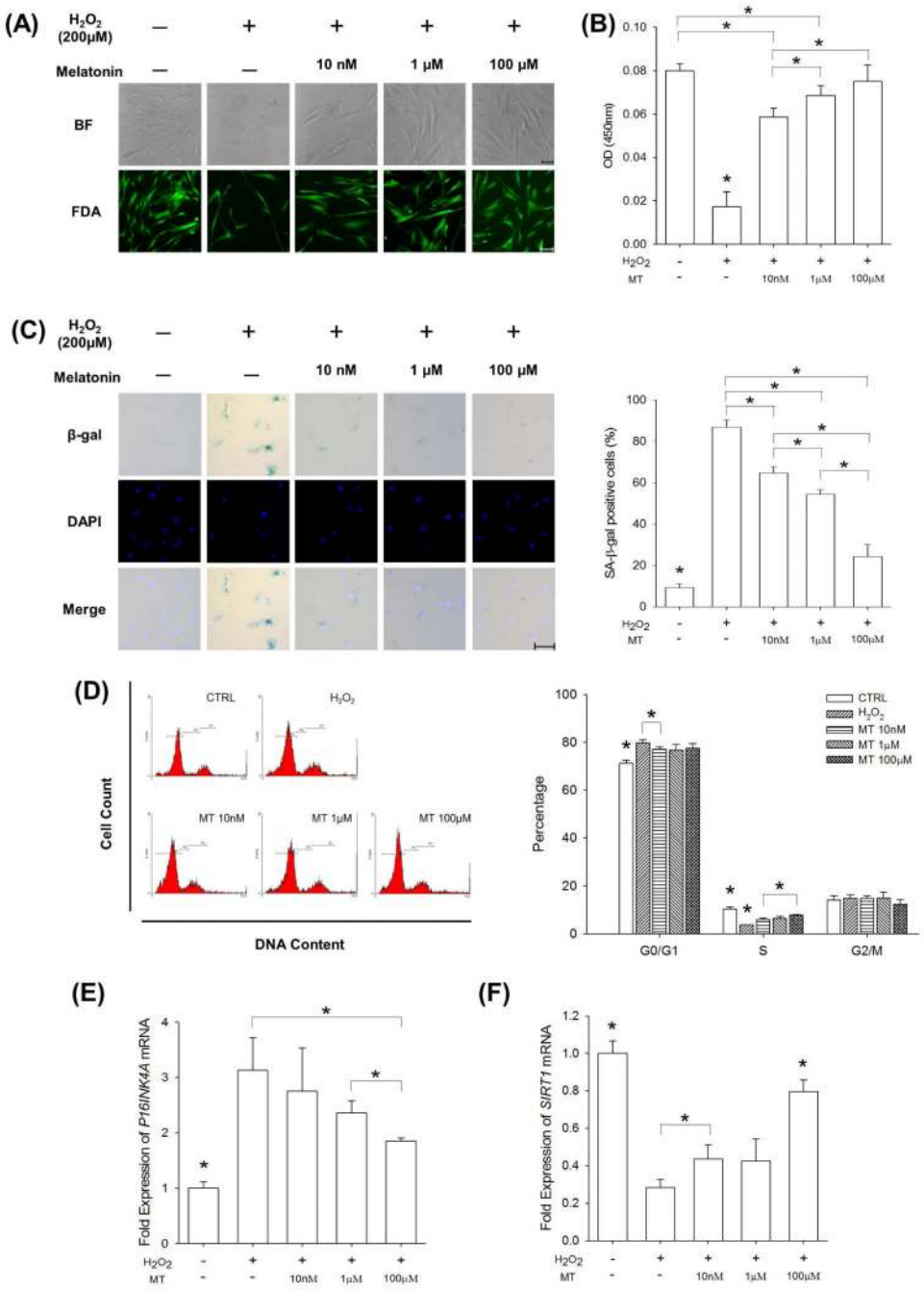

Fig. 4.

Treatment with melatonin reversed H_2O_2-induced premature senescence. BM-MSCs were treated with 200 μM H_2O_2 and subsequently with 10 nM, 1 μM, and 100 μM melatonin. (A) Cell morphology and density were observed in representative bright field (BF) images and fluorescence images labeled by fluorescein diacetate (FDA). Scale bar = 100 μm. (B) Cell proliferation was determined using the CCK-8 assay. Values are the mean ± S.E. of six independent experiments (n = 6). (C) Melatonin decreased the percentage of SA-β-gal-positive cells. Scale bar = 50 μm. (D) The cell cycle distribution was determined by flow

cytometry analysis. Values are the mean ± S.E. of three independent experiments ($n = 3$). The mRNA levels of *P16INK4A* (E) and *SIRT1* were measured by real-time RT-PCR. Values are the mean ± S.E. of four independent experiments ($n = 4$). Statistically significant differences are indicated by * ($p < 0.05$).

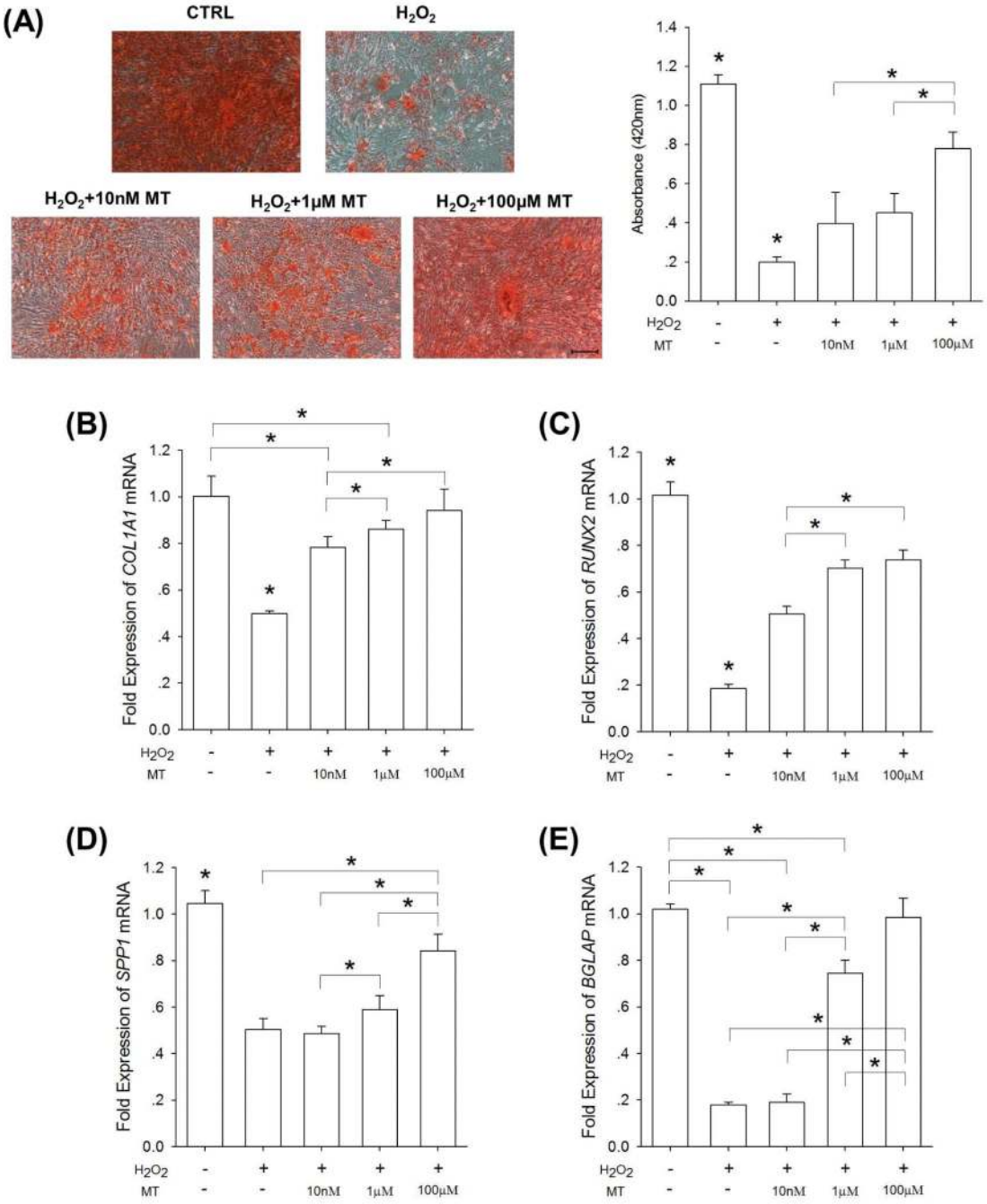

Fig. 5.

Treatment with melatonin restored senescence-inhibited osteogenic differentiation of BM-MSCs. Cells were treated with 200 μM H_2O_2 and incubated in osteogenic differentiation medium with or without the supplementation of melatonin. (A) Mineralization of the ECM was assessed by Alizarin Red S staining. Scale bar = 200 μm. The stained mineral layers were dissolved in 1% hydrochloric acid and were quantified via a spectrophotometer. Values are the mean ± S.E. of four independent experiments (n = 4). The mRNA levels of osteoblast-specific marker genes, including *COL1A1* (B), *RUNX2* (C), *SPP1* (D), and

BGLAP (E) were measured by real-time RT-PCR. Values are the mean ± S.E. of four independent experiments ($n = 4$). Statistically significant differences are indicated by * ($p < 0.05$).

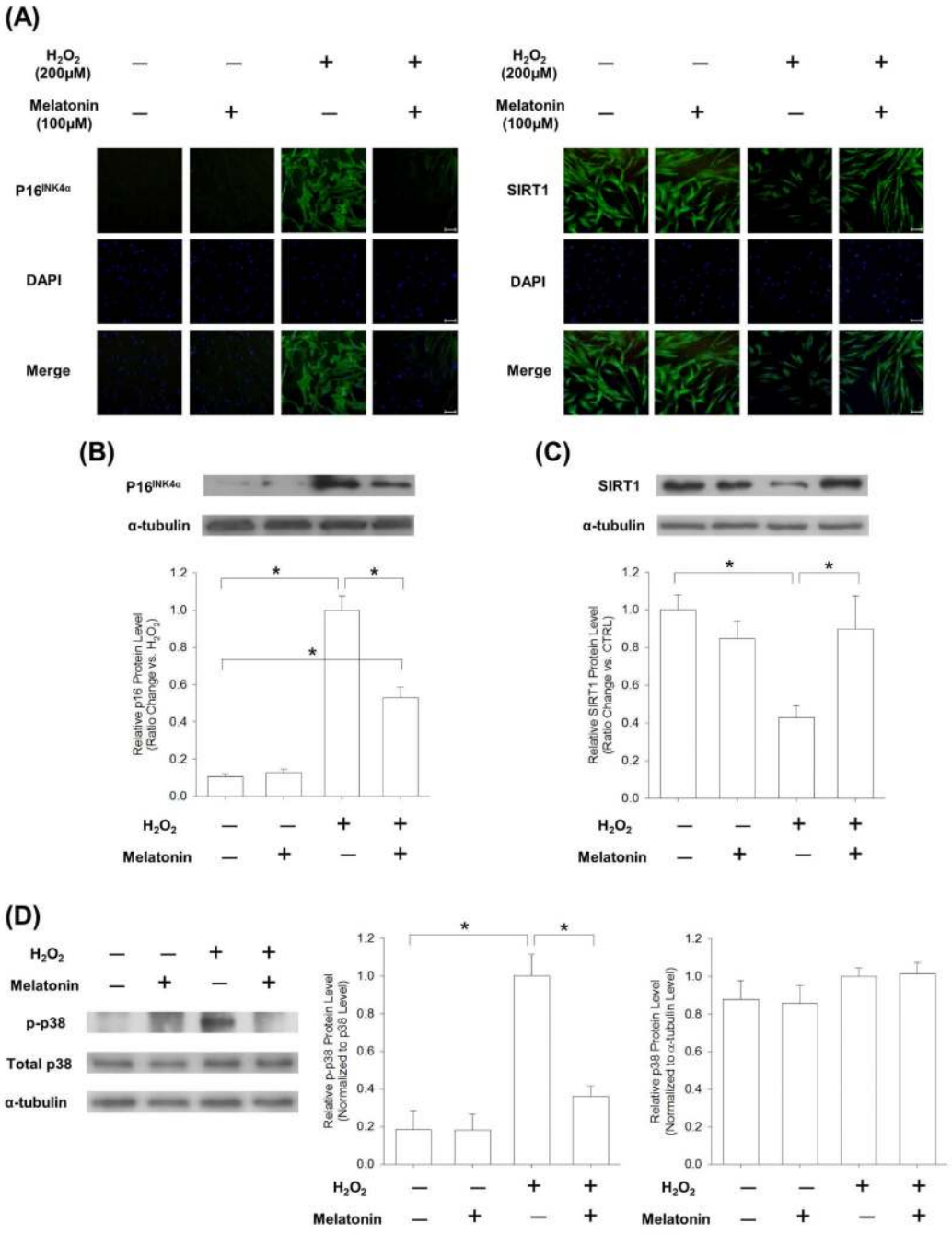

Fig. 6.

Melatonin mediated the SIRT1/p38/p16^{INK4α} pathway in senescent BM-MSCs induced by 200 μM H_2O_2. (A) Representative immunofluorescence staining images of BM-MSCs indicated that H_2O_2 treatment upregulated while melatonin attenuated p16^{INK4α} expression. Treatment with melatonin increased SIRT1 protein expression, which was suppressed by H_2O_2 treatment. Scale bar = 100 μm. Western blot analysis of p16^{INK4α} (B) and SIRT1 (C) expression in BM-MSCs confirmed the immunofluorescence results. The α-tubulin lane served as a loading control. (E) Western blot assay revealed activation of the p38 signaling

pathway by H_2O_2 treatment, whereas melatonin treatment attenuated phosphorylation of p38. The level of p-p38 was normalized to total p38 protein. The level of p38 was normalized to α-tubulin protein. Values are the mean ± S.E. of three independent experiments ($n = 3$). Statistically significant differences are indicated by * ($p < 0.05$).

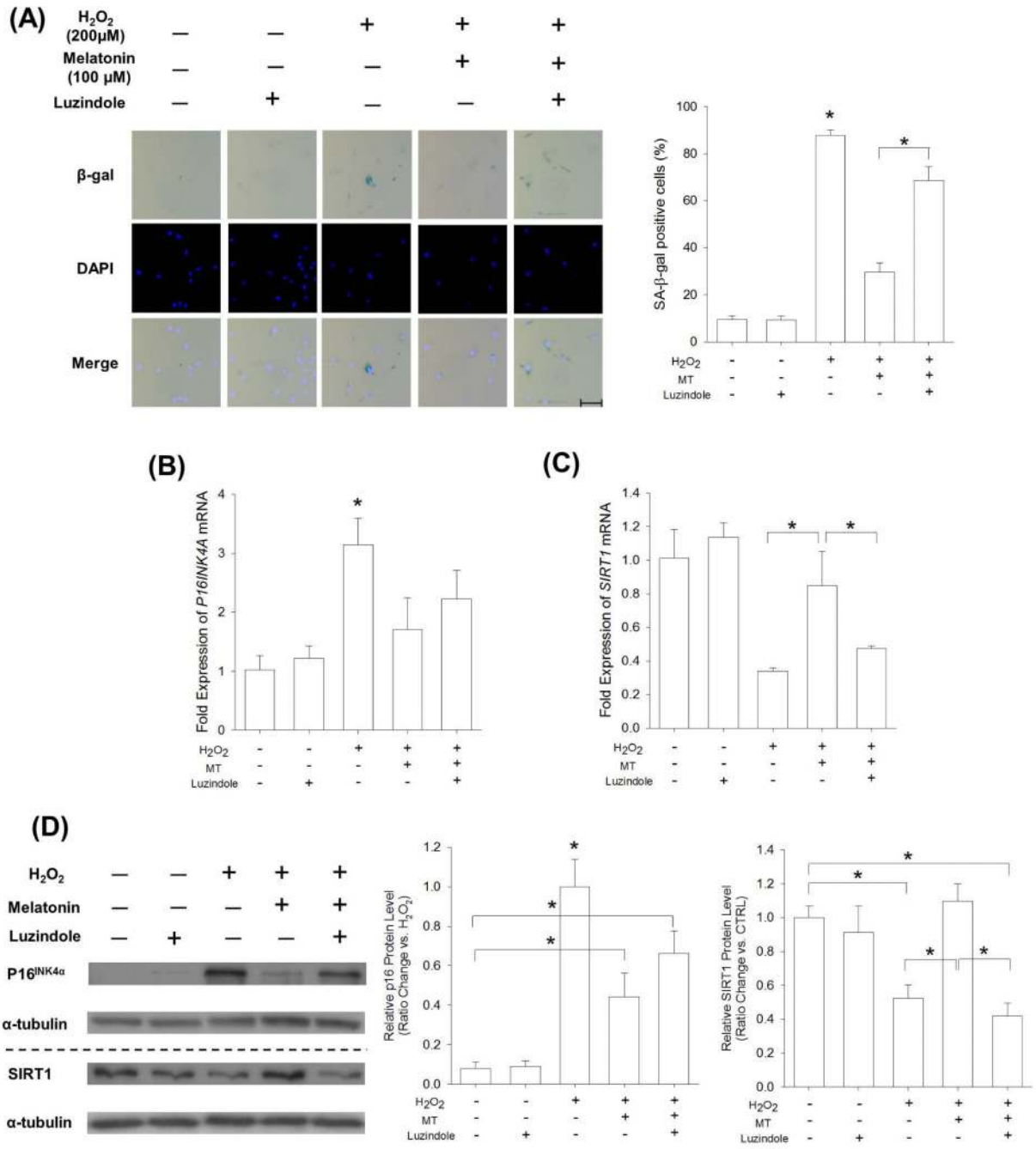

Fig. 7.

Luzindole inhibited the effects of melatonin on reversing premature senescence. BM-MSCs were treated with 200 μM H_2O_2 and subsequently with 100 μM melatonin or 10 μM luzindole. (A) Representative SA-β-gal (blue) staining images of BM-MSCs indicated senescent cells. Treatment with luzindole reversed melatonin-mediated inhibition of SA-β-gal-positive cells. Scale bar = 50 μm. The mRNA levels of *P16INK4A* (B) and *SIRT1* (C) were measured by real-time RT-PCR. Values are the mean ± S.E. of four independent experiments ($n = 4$). (D) Western blot analysis of $p16^{INK4\alpha}$ and SIRT1 protein expression in

BM-MSCs. Values are the mean ± S.E. of three independent experiments ($n = 3$). Statistically significant differences are indicated by * ($p < 0.05$).

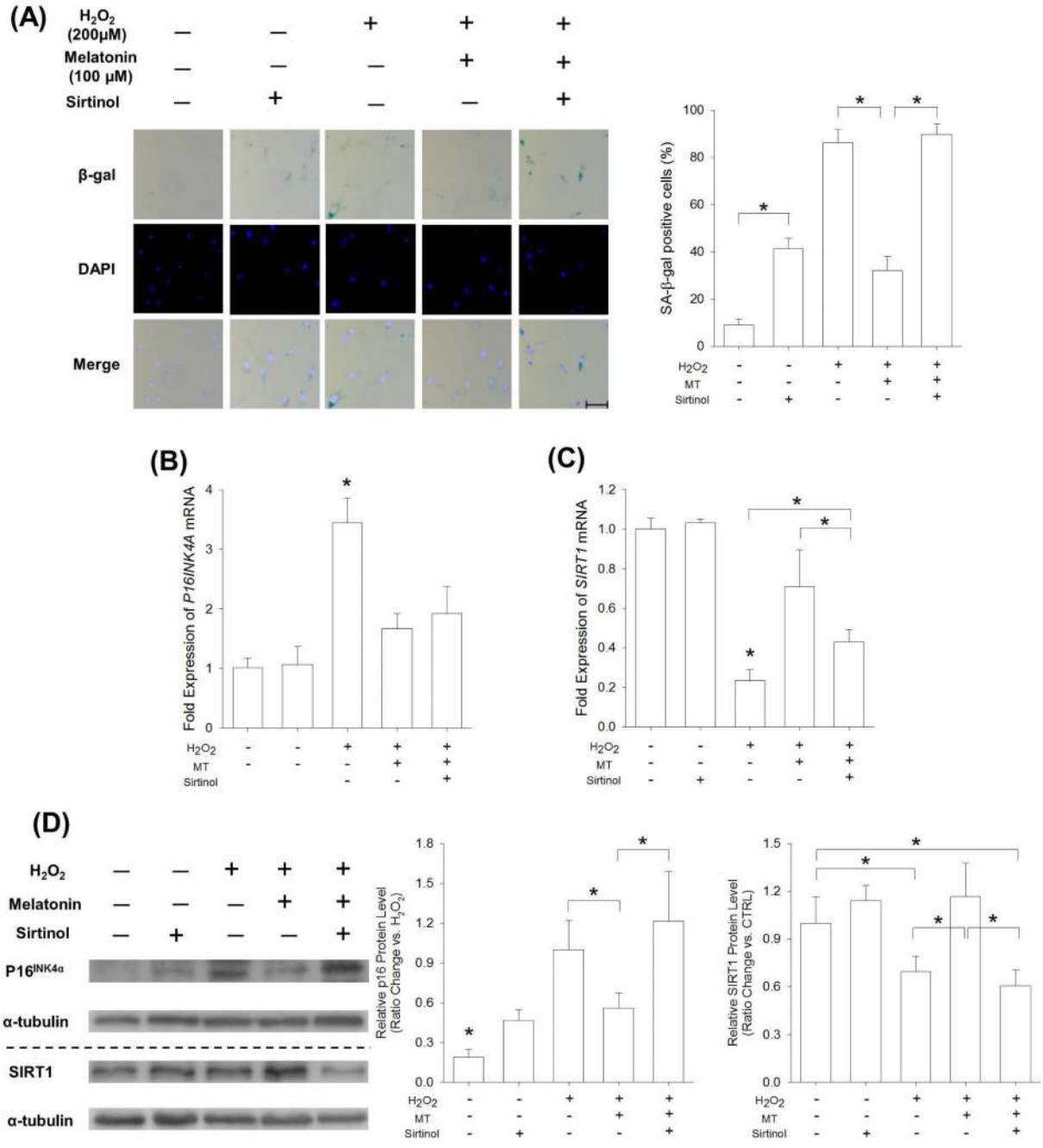

Fig. 8.

SIRT inhibition by sirtinol blocked melatonin-mediated anti-senescence effects. BM-MSCs were treated with 200 μM H_2O_2 and subsequently with 100 μM melatonin or 40 μM sirtinol. (A) Representative SA-β-gal (blue) staining images of BM-MSCs indicated senescent cells. Treatment with sirtinol reversed melatonin-mediated inhibition of SA-β-gal-positive cells. Scale bar = 50 μm. The mRNA levels of *P16INK4A* (B) and *SIRT1* (C) were measured by real-time RT-PCR. Values are the mean ± S.E. of four independent experiments (n = 4). (D) Western blot analysis of $p16^{INK4\alpha}$ and SIRT1 protein expression in BM-MSCs. Values are

the mean ± S.E. of three independent experiments ($n = 3$). Statistically significant differences are indicated by * ($p < 0.05$).

Table 1

Primers used for Real-time RT-PCR

Gene	Forward Primer sequence(5′-3′)	Reverse Primer sequence(5′-3′)
GAPDH	AGAAAAACCTGCCAAATATGATGAC	TGGGTGTCGCTGTTGAAGTC
P16INK4A	CCCAACGCACCGAATAGT	ATCTAAGTTTCCCGAGGTT
SIRT1	GCGGGAATCCAAAGGATAAT	CTGTTGCAAAGGAACCATGA
COL1A1	CAGCCGCTTCACCTACAGC	TTTTGTATTCAATCACTGTCTTGCC
RUNX2	AGAAGGCACAGACAGAAGCTTGA	AGGAATGCGCCCTAAATCACT
SPP1	GCGAGGAGTTGAATGGTG	CTTGTGGCTGTGGGTTTC
BGLAP	GAGCCCCAGTCCCCTACC	GACACCCTAGACCGGGCCGT